Proceedings of the Sixth International ASME Conference on Nanochannels, Microchannels and Minichannels
ICNMM2008
June 23-25, 2008, Darmstadt, Germany

ICNMM2008-62054

LOCAL MEASUREMENT OF FORCED CONVECTION HEAT TRANSFER IN A MICRO GLASS TUBE

B. Schilder
Department of Mechanical Engineering
Technische Universitaet Darmstadt
Germany

S. C. M. Yu
School of Mechanical
and Aerospace Engineering
Nanyang Technological University
Singapore

N. Kasagi
Department of Mechanical Engineering
The University of Tokyo
Japan

S. Hardt
Department of Mechanical
Engineering
University of Hanover
Germany

P. Stephan*
Department of Mechanical Engineering
Technische Universitaet Darmstadt
Germany
Email: pstephan@ttd.tu-darmstadt.de

ABSTRACT

The pressure drop and the convective heat transfer characteristics of ethanol and water in a 600 μm diameter tube with and without phase change has been studied experimentally. The test section consists of a glass tube coated with a transparent ITO (indium tin oxide) heater film. For single phase flow it was found that the measured Nusselt numbers and friction factors are in good agreement with the theoretical values expected from Poiseuille flow. Subsequently, the boiling heat transfer of ethanol was studied. It was found that boiling with bubble growth in both upstream and downstream directions leaving behind a thin evaporating liquid film on the tube wall is the dominant phase change process. Local Nusselt numbers are calculated for the two phase flow at different heat fluxes and Reynolds numbers. Compared to single phase flow the heat transfer is enhanced by a factor of 3 to 8.

NOMENCLATURE

c_p	specific heat $[J/(kg\,K)]$
d	tube diameter $[m]$
h	heat transfer coefficient $[W/(m^2K)]$
Δh_{lv}	latent heat of vaporization $[J/kg]$
I	electric current $[A]$
$\dot{M}$	mass flow rate $[kg/s]$
Nu	Nusselt number $[-]$
P	pressure $[Pa]$
$\dot{q}$	heat flux $[W/m^2]$
r	radius $[m]$
T	temperature $[^\circ C]$
t	time $[s]$
V	electric voltage $[V]$
x	axial distance $[m]$
χ	vapor quality $[\%]$
λ	thermal conductivity $[W/(m\,K)]$

SUBSCRIPTS

amb	ambiance
$elem$	element
$heat$	heating
in	inner
loc	local
$loss$	heat losses

*Address all correspondence to this author.

out	outer
th	thermocouple
$wall, in$	tube wall inside
$wall, out$	tube wall outside

INTRODUCTION

Heat and mass transfer in microchannels have been in the focus of intense research activities in the past decade due to their relevance in fields such as electronic equipment cooling and Lab-on-a-Chip technology. With regard to electronics, the heat flux density in microelectronic circuits has been constantly increasing, demanding more efficient cooling technologies. In this context, boiling heat transfer in microchannels or microtubes has been identified as a method for removing high heat fluxes. Despite the amount of research work in this area, conflicting results have been reported by different researchers around the globe. For example, the Nusselt numbers for single phase flow were found to vary from values less than the corresponding value for Poiseuille flow [1] to values three times higher than that. The friction factors for micro channels and tubes have also shown scattering results and many researchers attributed the effects to the surface conditions of the channels. A good summary of the topic can readily be found in the papers by Sobhan and Garimella [2], Palm [3] and more recently Morini [4]. The scatter of the experimental results may be in part due to difficulties associated with the experimental setup and the quantifications of uncertainty levels, the temperature measurements in particular. Due to the size of the tube considered, direct temperature measurements on the inner wall and in the liquid were not possible, they were normally derived from the measurements of outer wall temperature. Lelea et al. [5] and Celata et al. [6] are among the few who have shown results that are close to the classical theory value. Their experiments were conducted in a vacuum chamber to minimize heat losses.

For experiments involving phase changes, the prime interests would be on the visualization of the bubble formation process. In many of the experiments conducted previously, nucleate boiling, plug flow, slug flow and annular flow were identified as common flow patterns for microchannels and microtubes [7], [8]. In contrast to macro size tubes, these flow patterns are typically alternating with one another even at constant heat and mass fluxes in microtubes. Besides these well known flow patterns, unique microchannel patterns have also been described. Hetsroni et al. [9] found rapid bubble growth phenomena and called it explosive evaporation process due to high propagation velocity observed. Zhang et al. [10] postulate different boiling mechanisms depending on the channel size. For channels larger then 100 μm in diameter, they expect nucleate boiling as the major heat transfer process. In channels smaller 50 μm, they identified explosive boiling without bubble nucleation as being dominant. Hardt et al. [11] observed explosive boiling processes with subsequent film evaporation in channels with d_h = 50 μm and assumed bubble nucleation processes as a trigger to commence this process.

In the present investigation, an indium tin oxide (ITO) coated micro glass tube has been used for heat and mass transfer studies. The arrangement can effectively generate a uniform heat flux along the outer surface of the tube without providing optical obstruction to the test section. By employing a high speed camera, the liquid phase change at high heat fluxes could be visualized clearly.

EXPERIMENTAL ARRANGEMENT AND PROCEDURE

Figure 1 shows a schematic view of the experimental rig used in the present investigation. Distilled and degassed water and degassed ethanol are used as the working fluids for the convective heat transfer experiments. The working fluid is delivered to the test section via a micro pump. The flow rate is accurate to within +/- 1 %. Experiments have been carried out in the range of the inlet Reynolds number of 25-600. The fluid temperatures before and after the glass tube (T_{in} and T_{out}) are measured by 0.5 mm diameter K-type thermocouples in the inlet and outlet mixing blocks. K-type thermocouples with a diameter of 25 μm are used for the measurement of the temperatures along the tube (T_0-T_7). These thermocouples are glued by silicone with at thermal conductivity of 1.53 $W/(mK)$ to the outer wall of the tube. All thermocoupels are calibrated for the experimental temperature range and have an accuracy of +/- 0.1 K. Pressure measurements are performed by a Sokken Pz-77 pressure transducer with an accuracy of +/- 98.1 Pa. The flow visualization is conducted via a high speed camera (Vision Research Phantom V5.0) operated

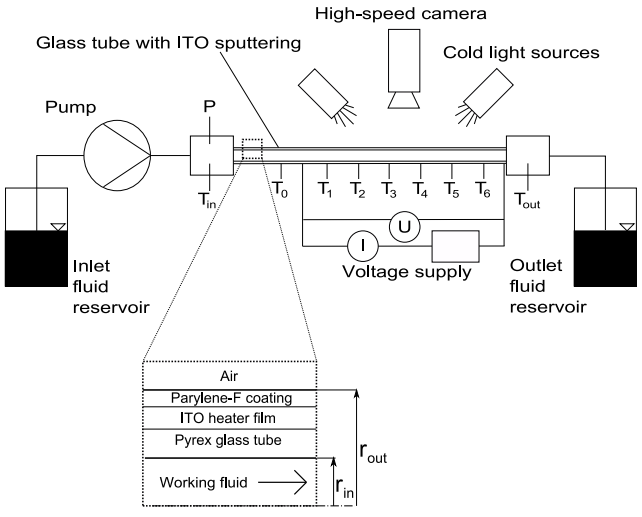

Figure 1. SCHEMATIC VIEW OF THE EXPERIMENTAL RIG.

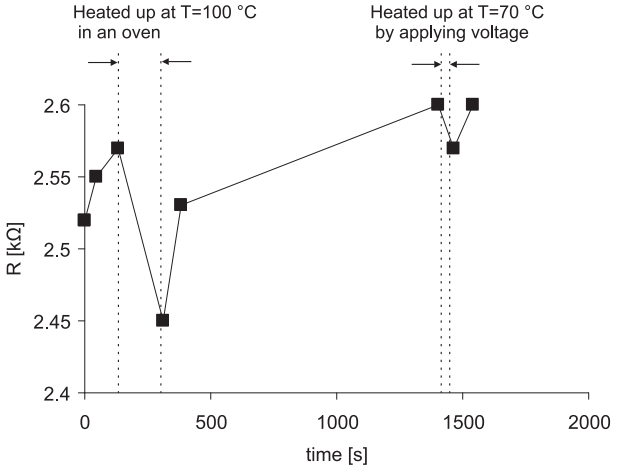

Figure 2. CHANGE OF ELECTRIC RESISTANCE OF UNPROTECTED ITO FILM.

at a frame rate of up to 8100 per second and an interrogation area of 1024 x 1024 pixels. The glass tube test section is a 600 μm internal diameter tube (outer diameter 1000 μm) with a rather smooth inner surface, only shallow cavities with a diameter of 2-5 μm could be identified. The outer surface of the glass tube is coated with a 2 μm ITO/Ag film such that Joule heating can be applied uniformly along the coated surface, which remains transparent. The uniformity of the electric resistance of the ITO film is within +/- 5 %. Silver paste with a specific electric resistance of $5 \cdot 10^{-5}\ \Omega\, cm$ is used to connect the copper wires to the ITO film to supply electric current. It became evident that the ITO film is sensitive to oxidation. Figure 2 shows the electric resistance over time for the unprotected ITO film in the vicinity of air. Without heating the electric resistance is monotonously increasing; but if the film is exposed to external heating or Joule heating is applied, it decreases. Therefore, we protected the ITO film from the enviromental oxygen by a 0.42 μm Parylene-F coating to avoid oxidation. A constant heat flux is supplied along the outer surface of the tube by applying a constant voltage between the two wires connected to the test section. The heating is stable to within +/- 2 % over a period of six hours. The total length of the glass tube is 200 *mm*, of which a section of 110 *mm* is heated. The entry length in front of the heated section is 85 *mm* long to ensure hydrodynamically developed flow.

The experiments were conducted as follows. The working fluid is fed to the test section at room temperature (T = 23 $°C$). The flow rate of the working fluid and the heating voltage were fixed at the desired values. To assure a steady state condition, the measurement data were taken after a waiting time of 20 minutes. Temperature and pressure data was recorded in real time every 464 *ms*. The recorded data of 40 measurement cycles were averaged for calculating the Nusselt number and friction factor.

DATA REDUCTION AND UNCERTAINTIES

Estimation of heat losses

Preliminary experiments with an empty test section were conducted to estimate heat losses due to free convection, conduction and radiation. The heat transfer coefficient of the heat losses is defined as:

$$h_{loss} = \frac{\dot{q}_{loss}}{T_{wall,out} - T_{amb}} \tag{1}$$

Due to the fact that no working fluid is employed in the preliminary case, the joule heating is transfered to the ambiance:

$$\dot{q}_{loss} = \dot{q}_{heat} = \frac{V\, I}{\pi\, d_{out}\ l_{heat}} \tag{2}$$

where V and I are the voltage and the current measured at the copper wires connected to the tube, d_{out} is the outer diameter of the tube and l_{heat} is the heated length. The experimentally estimated h_{loss} has been compared to calculations following Nusselt number correlations for natural convection at the wall of a horizontal cylinder [12]. Depending on the tube temperature, the experimentally derived h_{loss} is up to 40 % higher than the theoretical value for convection only. Additional heat losses due to radiation and conduction (axial along the tube and via the thermocouple and heater wires) are the likely reasons for this discrepancy. Nevertheless, it was found that the heat losses are less than 10 % of the total heat input for all experiments with working fluid.

A second order polynomial is used to provide a continuous relationship for q_{loss} depending on $T_{wall,out} - T_{amb}$:

$$\dot{q}_{loss} = (T_{wall,out} - T_{amb})^2 \cdot c_1 + (T_{wall,out} - T_{amb}) \cdot c_2 + c_3 \tag{3}$$

c_1, c_2, c_3 are the coefficients that fit the experimental data best in a least-squares sense.

Calculation of local heat transfer performance

The local heat transfer performance for single phase and two phase flow between the inside wall of the tube and the working fluid is expressed by the dimensionless Nusselt number. The local Nusselt number is calculated for all thermocouple positions at the heated length of the tube:

$$Nu_{loc} = \frac{h_{loc} \cdot d_{in}}{\lambda_{liquid}} \tag{4}$$

The thermal conductivity of the pure liquid λ_{liquid}, either ethanol or water, and the inner diameter of the tube have been used for calculating Nu_{loc} for single phase and two phase flow.

The local heat transfer coefficient is given as:

$$h_{loc} = \frac{\dot{q}_{loc}}{T_{wall,in} - T_{bulk}} \tag{5}$$

When pumping a working fluid through the tube, a part of the heat is transfered into the working fluid and another part to the ambiance. The heat transfered to the working fluid is calculated as follows:

$$\dot{q}_{loc} = \dot{q}_{heat} - \dot{q}_{loss} \tag{6}$$

$$\dot{q}_{loc} = \frac{V\,I}{\pi\, d_{in}\, l_{heat}} - \dot{q}_{loss} \tag{7}$$

$\dot{q}_{loss}$ is calculated depending on the measured temperatures using Eqn. (3). Due to the constant electric resistance of the ITO film along the tube, $\dot{q}_{heat}$ is constant over the total heated area. The heat loss $\dot{q}_{loss}$ is a function of the temperature difference $T_{wall,out} - T_{amb}$, which is changing along the heated tube due to the heat transfer to the working fluid. Therefore, $\dot{q}_{loss}$ and $\dot{q}_{loc}$ are functions of the axial distance x.

The temperature at the inner wall of the tube at each thermocouple position is computed using the one-dimensional heat conduction equation in cylindrical coordinates:

$$T_{wall,in} = T_{wall,out} - \frac{\dot{q}_{loc} \cdot d_{in}}{2 \cdot \lambda_{tube}} ln \frac{d_{out}}{d_{in}} \tag{8}$$

The axial conduction number introduced by Maranzana et al. [13], has been calculated to find out whether the assumption of one-dimensional heat transfer is reasonable. According to Maranzana axial conduction can be neglected if the conduction number is lower than 10^{-2}. Depending on the flow rate we found $4.0 \cdot 10^{-6}$...$4.8 \cdot 10^{-5}$.

The average fluid temperature, referred to as bulk temperature, is calculated for each thermocouple position by taking the energy balances:

$$T_{bulk} = T_{in} + \frac{1}{x} \int_0^{x_{th}} \dot{q}_{loc}\, dx \cdot \frac{\pi\, d_{in}\, x_{th}}{\dot{M}\, c_p} \tag{9}$$

where x_{th} is the axial distance of the thermocouple measured from the starting point of the heated length. For the calculation the heated length of the tube has been discretized with 110 cylindrical elements with an increment of 1 *mm*. For experiments where boiling has been observed, the maximum bulk temperature is specified as the saturation temperature of the liquid. The saturation pressure inside the tube is calculated by linear interpolation between inlet block pressure and ambient pressure.

The heat transfered from each element to the working fluid is then calculated in the same way as the local heat flux (Eqn. (7)). The heat losses from the elements are estimated by using Eqn. (3).

The mean outside wall temperature of the elements is interpolated by a third order polynomial. The coefficients of the polynomial are found by fitting the polynomial to the temperatures measured by the micro thermocouples at the outside wall of the tube.

The local vapor quality for each measurement point is calculated as:

$$\chi = \frac{1}{x} \int_0^{x_{th}} \dot{q}_{loc}\, dx \cdot \frac{\pi\, d_{in}\, x_{th}}{\dot{M}\, \Delta h_{lv}} - \frac{c_p \cdot (T_{bulk} - T_{in})}{\Delta h_{lv}} \tag{10}$$

The temperature dependent fluid properties such as viscosity, density, thermal conductivity and specific heat are defined for each measurement point based on the bulk temperature calculated by Eqn. (9). The equivalent wall heat flux due to heating of the liquid by viscous dissipation has been calculated to be less than 40 W/m^2 which is in all cases less than 1 % of the joule heating, and thus has been neclected.

The standard deviation of the Nusselt number due to the measurement uncertainties is calculated following the Gaussian error propagation formula to less then $\frac{\Delta Nu}{Nu} = \pm 20\%$ for all test runs.

RESULTS AND DISCUSSION

Single phase

The pressure drop for distilled water and ethanol was measured in the whole range of inlet Reynolds numbers in which heat transfer experiments were conducted. The derived friction factor is well in agreement with the theory for laminar flow (friction factor = 64/*Re*) (Fig. 3). Since the inlet pressure is measured before the fluid enters the microtube, entrance effects seem to be negligible.

Figure 4 shows the typical temperature distribution for a single phase test run. The wall temperatures and the bulk temperatures are almost on parallel lines indicating that the heat flux generated is uniformly distributed along the surface and heat losses are marginal. Figure 5 shows the local Nusselt numbers for two Reynolds numbers and six different heat fluxes. They converge towards the classical value for constant heat flux and Poiseuille flow (Nu = 4.36) at about 80 % of the heated tube length. Higher Nusselt numbers at the entrance to the heated section are a consequence of thermal entrance effects. Grigull and Tratz [14] investigated the thermal entrance problem for laminar flow with constant heat flux numerically and evaluated the Nusselt number

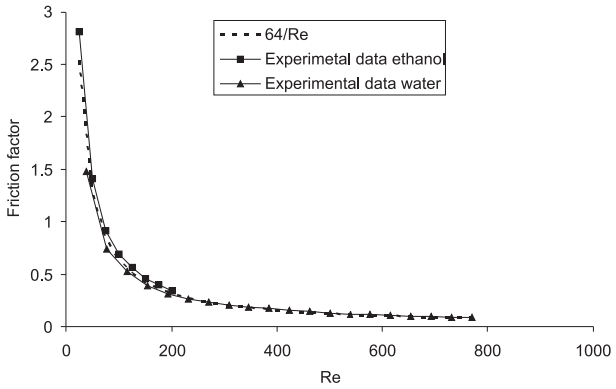

Figure 3. FRICTION FACTOR COMPARED TO THEORY FOR LAMINAR FLOW.

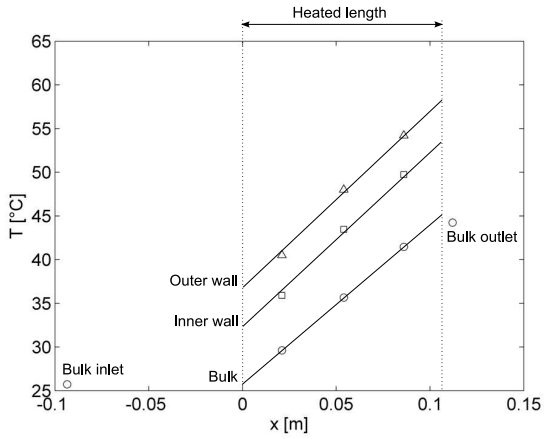

Figure 4. OUTER WALL, INNER WALL AND BULK TEMPERATURE.

as a function of the dimensionless axial distance $(x/(d\,Re\,Pr))$. In Fig. 6 the data of multiple test runs using water and ethanol is compared with the correlation of Grigull and Tratz. If the experimental uncertainties are accounted for, the present measurements agree with the classical theory. The results imply that momentum and heat transfer for single phase flow in microtubes are well described by the standard correlations.

Boiling

Boiling experiments have been conducted with ethanol as a working fluid. Alternating flow patterns with a defined sequence have been observed. A typical evaporation cycle starts with a single bubble nucleation process. At first the bubble is growing comparatively slowly, but once the bubble diameter reaches the inner diameter of the tube, the bubble growth rate is strongly enhanced. Constricted by the tube wall, the bubble grows in streamwise direction as well as in counter streamwise direction. Depending on the heat flux and the inlet Reynolds number, even

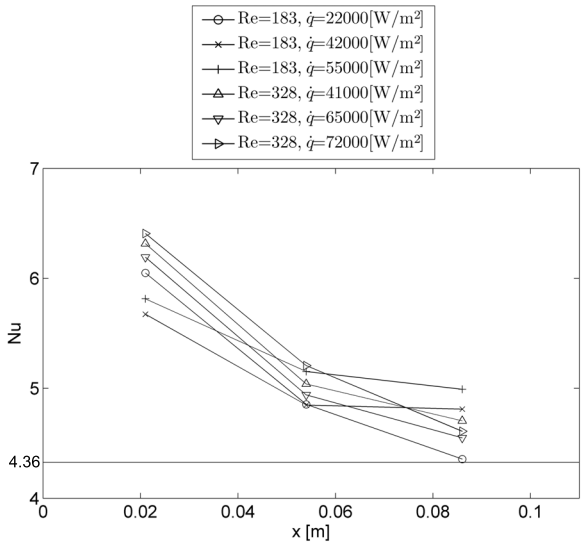

Figure 5. NUSSELT NUMBER VARIATION IN FLOW DIRECTION FOR SINGLE PHASE HEAT TRANSFER.

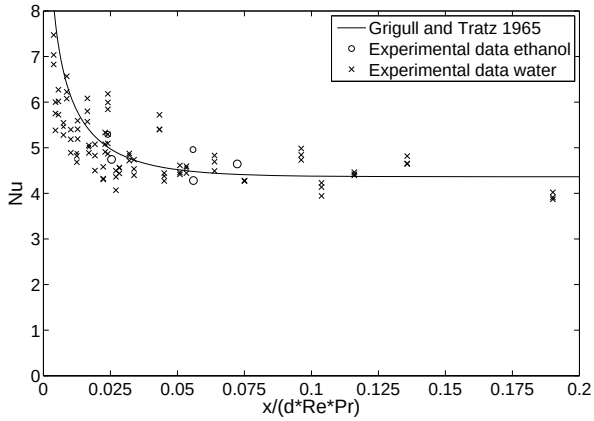

Figure 6. NUSSELT NUMBER, EXPERIMENTAL RESULTS COMPARED TO CORRELATION OF GRIGULL AND TRATZ FOR SINGLE PHASE HEAT TRANSFER.

the tube area upstream of the heated section is affected by two phase flow pattern due to counter streamwise bubble growth. A liquid film is formed between the growing bubble and the tube wall. Due to evaporation the liquid film thickness decreases. If the time period before the next liquid plug arrives is long, the liquid film ruptures and dryout occurs. Photographic images of the described cyclic evaporation process are displayed in Fig. 7 where a typical evaporation cycle starting with a bubble nucleation event in the camera's field of view is shown. The pictures were taken at a Reynolds number of 86 and a heat flux of 66000 W/m^2 between the 4th and the 5th thermocouple in the heated

area with a resolution of 1000 fps.

- t = 0 ms: Two vapor bubbles are detached from the heated wall and transported with the liquid.
- t = 3 ms: The bubbles are growing. Once the diameter of a bubble equals the channel diameter, the bubble is growing faster than before (right bubble compared to left bubble).
- t = 7 ms: The left bubble has reached the channel diameter and is expanding in streamwise direction. Liquid is pressed to the channel wall due to the fast bubble growth forming a thin liquid film between bubble and wall. The right bubble has left the camera's view field.
- t = 16 ms: The bubble starts to grow in counter streamwise direction as well. The smallest liquid film thickness is found at the location of first contact of the bubble with the wall of the tube (indicated by an arrow).
- t = 30 ms: During the growth in counter streamwise direction the liquid film thickness is decreasing and a film rupture takes place (indicated by arrows).
- t = 59 ms: Liquid is refilling the tube and pushing the bubble out of the camera's field of view in streamwise direction.

By utilizing flow visualization, thin film evaporation triggered by single bubble nucleation could be identified as the dominant phase change process.

High pressure fluctuations induced by the unsteady evaporation process have been measured. Figure 8 shows the change of pressure drop for the transition from single phase heat transfer to boiling at t = 2652 s in a test run. The pressure drop suddenly jumps from a virtually constant value of 3300 Pa for single phase flow to a fluctuating value of 8000-12000 Pa for the previously described boiling process. The cyclic flow pattern, especially the upstream bubble growth, is the reason for the strong pressure fluctuations.

Compared to the single phase experiments the heat transfer performance is considerably enhanced by boiling. Figures 9, 10 and 11 show the time averaged local Nusselt numbers as a function of vapor quality for three different inlet Reynolds numbers. In all cases, the liquid temperature at the first thermocouple in the heated area is significantly lower than the saturation temperature of the liquid, so that the vapor quality for the first measured local Nusselt number is equal to zero. Nevertheless, compared to the single phase experiments the heat transfer is enhanced even at a position where no boiling occurs. Since bubble growth in counter streamwise direction is observed, this effect is supposed to be the reason for heat transfer enhancement upstream of the position where the saturation temperature is reached.

For Re = 86, the local Nusselt numbers for boiling are about 20 and seem to be independent of the vapor quality and the heat flux in the tested range (Fig. 9.). For higher Reynolds numbers higher local Nusselt numbers were measured. At Re = 128 and 171, the average local Nusselt numbers are about 27, and

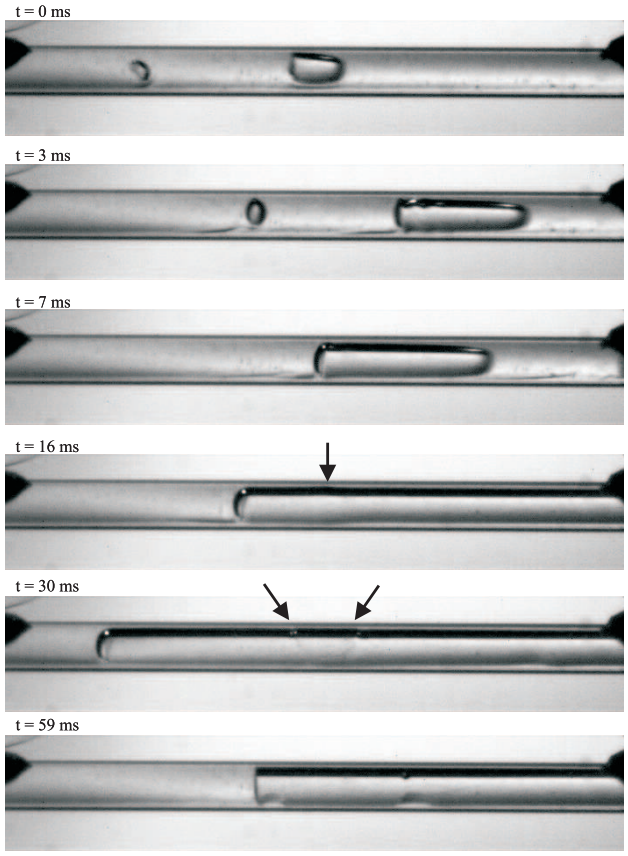

Figure 7. EVOLUTION OF FLOW PATTERN DURING A BOILING CYCLE.

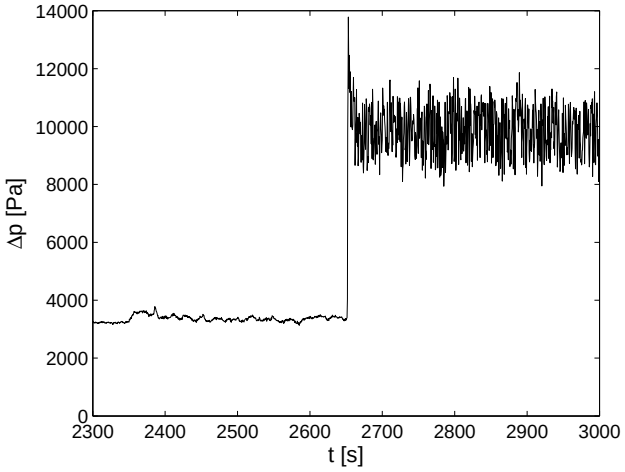

Figure 8. PRESSURE DROP, TRANSITION FROM SINGLE PHASE FLOW TO BOILING. Re = 128, $\dot{q}$ = 79000 $W/(mK)$.

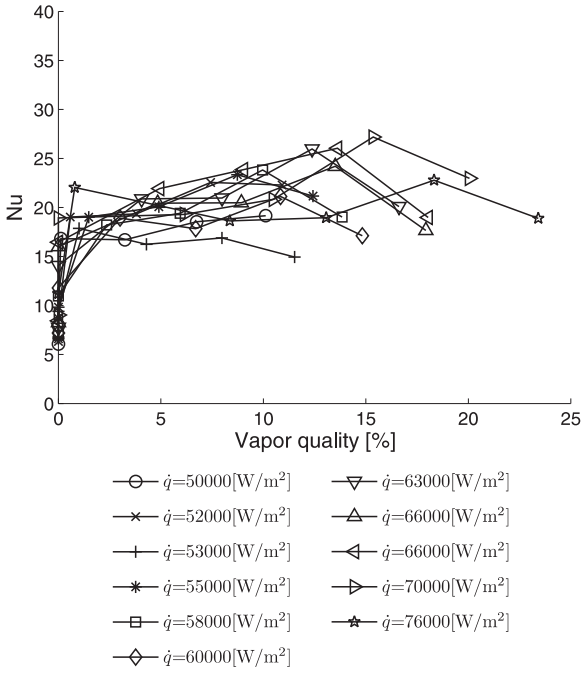

Figure 9. NUSSELT NUMBERS FOR BOILING. *Re* = 86.

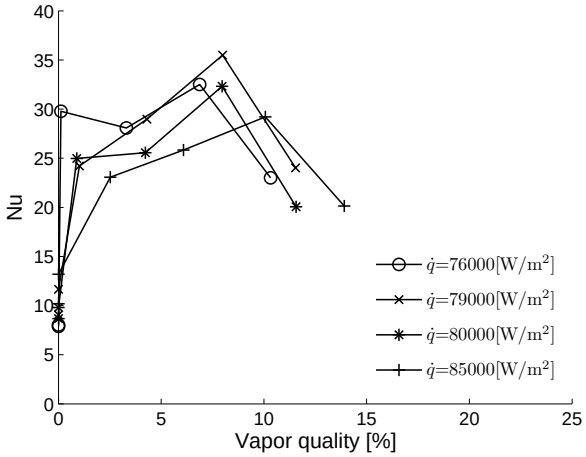

Figure 10. NUSSELT NUMBERS FOR BOILING. *Re* = 128.

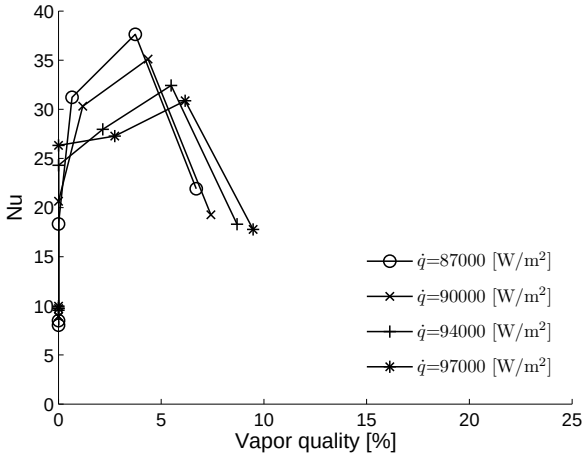

Figure 11. NUSSELT NUMBERS FOR BOILING. *Re* = 171.

a dependency on the vapor quality could be observed. While at the last thermocouple the local Nusselt number is about 20 in all cases, the Nusselt numbers are increasing with increasing Reynolds number for the other thermocouples at lower vapor quality. Dryout phenomena could be the reason for the reduced heat transfer performance at the end of the tube in Figures 10 and 11, but the vapor qualities are lower than that for *Re* = 86 (Fig. 9). Nevertheless, alternating flow patterns may trigger a long dryout time fraction even at a low mean vapor quality if, for example, the time fraction for which liquid plugs are present is also comparatively long. As a consequence, the two-phase flow pattern responsible for high heat transfer performance might be largely suppressed.

The dependency of the heat transfer performance on heat flux is rather unpronounced. Only at *Re* = 171 a tendency could be identified, the local Nusselt number is slightly decreasing with increasing heat flux, but the deviation is within the measurement uncertainty of $\pm$ 20 % (Fig. 10). In common flow boiling models the heat transfer is divided into two parts: nucleate boiling heat transfer and convective boiling heat transfer. The nucleate boiling heat transfer performance is know to be a function of heat flux, while the convective heat transfer is found to be rather independent of it, but a function of mass velocity [15]. Thus, the behavior of the local Nusselt numbers supports the impression obtained by flow visualization, namely that nucleate boiling is not the dominant heat transfer process in our experiments. Qu and Mudawar [16] studied flow boiling of water in parallel microchannels and concluded that forced convection boiling is the dominant heat transfer mechanism in their heat sink. Comparable to our studies, they found that the saturated flow boiling heat transfer coefficient is a function of mass velocity and only a weak function of heat flux. However, in our experiments an increase of the Reynolds number only slightly enhances the heat transfer performance. While Qu and Mudawar employed water in their boiling experiments, we used ethanol which has a higher viscosity. The lower fluidity of ethanol may decrease the dependency of the heat transfer performance on the Reynolds number.

Thome et al. [17] developed a model to predict the heat transfer performance of boiling processes in microchannels and found rather good agreement with the experimental database [18]. In their model, counter streamwise bubble growth is not

considered and the heat transfer performance is a function of the heat flux. Our results indicate that refined models are needed to account for the phenomena observed in our experiments.

CONCLUSION

Experiments were conducted to determine friction factors and Nusselt numbers in a microtube with an inner diameter of 600 μm. Distilled water and ethanol were used as the working fluids. The major findings from the study are summarized as follows:

- The friction factor and the Nusselt number for single phase flow with constant heating agree with the classical theories for laminar flow (friction factor = $64/Re$, $Nu = 4.36$ for constant heat flux).
- For boiling, alternating flow patterns with a defined sequence have been observed. Evaporation of a thin liquid film covering the tube wall seems to be the dominant heat transfer mechanism.
- The mean pressure drop for boiling is about 3 times higher than that for single phase flow. Due to the fast alternating flow patterns the pressure drop is fluctuating in a range of about $\pm$ 10 %.
- The Nusselt number for boiling is: independent of the heat flux, increasing with increasing Reynolds number, and up to eight times higher than that for single phase heat transfer.

ACKNOWLEDGMENT

We thank Prof. Suzuki for valuable discussions and Mr. Hamana, Mr. Hayashi and Mr. Miwa for technical assistance. Boris Schilder received support for this project as a JSPS Scientific Visitor to the Turbulence and Heat Transfer Laboratory at The University of Tokyo.

REFERENCES

[1] Shah, R. K., and London, A. L., 1978. *Laminar flow forced convection in ducts : a source book for compact heat exchanger analytical data*. Academic Press.

[2] Sobhan, C. B., and Garimella, S. V., 2001. "A comparative analysis of studies on heat transfer and fluid flow in microchannels". *Microscale Thermophysical Engineering*, **5**(4), Oct-Dec, pp. 293–311.

[3] Palm, B., 2001. "Heat transfer in microchannels". *Microscale Thermophysical Engineering*, **5**(3), pp. 155–175.

[4] Morini, G. L., 2004. "Single-phase convective heat transfer in microchannels: a review of experimental results". *International Journal of Thermal Sciences*, **43**(7), pp. 631–651.

[5] Lelea, D., Nishio, S., and Takano, K., 2004. "The experimental research on microtube heat transfer and fluid flow of distilled water". *International Journal Of Heat And Mass Transfer*, **47**(12-13), Jun, pp. 2817–2830.

[6] Celata, G. P., Cumo, M., Marconi, V., McPhail, S. J., and Zummo, G., 2006. "Microtube liquid single-phase heat transfer in laminar flow". *International Journal of Heat and Mass Transfer*, **49**(19-20), Sep, pp. 3538–3546.

[7] Gasche, J. L., 2006. "Carbon dioxide evaporation in a single microchannel". *Journal of the Brazilian Society of Mechanical Sciences and Engineering*, **28**, pp. 69–83.

[8] Yen, T. H., Shoji, M., Takemura, F., Suzuki, Y., and Kasagi, N., 2006. "Visualization of convective boiling heat transfer in single microchannels with different shaped cross-sections". *International Journal Of Heat And Mass Transfer*, **49**(21-22), Oct, pp. 3884–3894.

[9] Hetsroni, G., Mosyak, A., Pogrebnyak, E., and Segal, Z., 2005. "Explosive boiling of water in parallel microchannels". *International Journal of Multiphase Flow*, **31**(4), Apr, pp. 371–392.

[10] Zhang, L. A., Wang, E. N., Goodson, K. E., and Kenny, T. W., 2005. "Phase change phenomena in silicon microchannels". *International Journal of Heat and Mass Transfer*, **48**(8), Apr, pp. 1572–1582.

[11] Hardt, S., Schilder, B., Tiemann, D., Kolb, G., Hessel, V., and Stephan, P., 2007. "Analysis of flow patterns emerging during evaporation in parallel microchannels". *International Journal of Heat and Mass Transfer*, **50**(1-2), Jan, pp. 226–239.

[12] Verein Deutscher Ingenieure, 1991. *Wärmeatlas*, 6., erw. aufl. ed. VDI-Verl.

[13] Maranzana, G., Perry, I., and Maillet, D., 2004. "Mini- and micro-channels: influence of axial conduction in the walls". *International Journal Of Heat And Mass Transfer*, **47**(17-18), Aug, pp. 3993–4004.

[14] Grigull, U., and Tratz, H., 1965. "Thermischer einlauf in ausgebildeter laminarer rohrströmung". *International Journal of Heat and Mass Transfer*, **8**(5), p. 669.

[15] Thome, J. R., and Collier, J. G., 1996. *Convective boiling and condensation*, 3rd ed. Clarendon Press.

[16] Qu, W., and Mudawar, I., 2003. "Flow boiling heat transfer in two-phase micro-channel heat sinks–i. experimental investigation and assessment of correlation methods". *International Journal of Heat and Mass Transfer*, **46**(15), p. 2755.

[17] Thome, J. R., Dupont, V., and Jacobi, A. M., 2004. "Heat transfer model for evaporation in microchannels. part i: presentation of the model". *International Journal of Heat and Mass Transfer*, **47**(14-16), Jul, pp. 3375–3385.

[18] Dupont, V., Thome, J. R., and Jacobi, A. M., 2004. "Heat transfer model for evaporation in microchannels. part ii: comparison with the database". *International Journal of Heat and Mass Transfer*, **47**(14-16), Jul, pp. 3387–3401.